symmetry

IMPACT FACTOR 2.2

CITESCORE 5.4

Review

The Neutron Lifetime Discrepancy and Its Implications for Cosmology and Dark Matter

Fred E. Wietfeldt

Special Issue
The Dark Universe: The Harbinger of a Major Discovery

Edited by
Prof. Konstantin Zioutas

MDPI

https://doi.org/10.3390/sym16080956

symmetry

MDPI

Review

The Neutron Lifetime Discrepancy and Its Implications for Cosmology and Dark Matter

Fred E. Wietfeldt

Department of Physics and Engineering Physics, Tulane University, New Orleans, LA 70118, USA; few@tulane.edu

Abstract: Free neutron decay is the prototype for nuclear beta decay and other semileptonic weak particle decays. It provides important insights into the symmetries of the weak nuclear force. Neutron decay is important for understanding the formation and abundance of light elements in the early universe. The two main experimental approaches for measuring the neutron lifetime, the beam method and the ultracold neutron storage method, have produced results that currently differ by 9.8 ± 2.0 s. While this discrepancy probably has an experimental origin, a more exciting prospect is that it may be explained by new physics, with possible connections to dark matter. The experimental status of the neutron lifetime is briefly reviewed, with an emphasis on its implications for cosmology, astrophysics, and dark matter.

Keywords: neutron decay; neutron lifetime; beta decay

Citation: Wietfeldt, F.E. The Neutron Lifetime Discrepancy and Its Implications for Cosmology and Dark Matter. *Symmetry* **2024**, *16*, 956. https://doi.org/10.3390/sym16080956

Academic Editors: Abraham A. Ungar and Alberto Ruiz Jimeno

Received: 6 June 2024
Revised: 8 July 2024
Accepted: 18 July 2024
Published: 26 July 2024

1. Introduction

The neutron is an ubiquitous particle in the world around us. The atomic nuclei of all atoms except for light hydrogen contain neutrons. In a stable nucleus, the energy associated with nuclear structure prevents neutrons and protons from decaying via the weak force, but a free neutron may decay because its rest energy exceeds that of the particles in their final state. This process, where a free neutron decays into a proton, electron, and antineutrino with a mean lifetime of about 880 s, is the simplest example of nuclear beta decay. It has important consequences in cosmology and astrophysics. While the dynamical theory of the Standard Model of particle physics is well established, currently available theoretical methods are not able to accurately calculate the neutron decay lifetime. The neutron lifetime has been measured in many major experiments over the past 75 years. Two very different methods have dominated these measurements: free neutron beam experiments and ultracold neutron storage experiments. Unfortunately, the most precise versions of these experiments disagree by about 10 s, a discrepancy of almost five standard deviations. This is most likely due to unknown systematic effects in one or more of the experiments, but it is conceivable that new physics is responsible, which would have many important ramifications.

2. Theoretical Discussion

Free neutron decay is a manifestation of the charged current weak interaction whereby a negatively charged down quark is transformed into a positively charged up quark, emitting a charged W boson that immediately decays into an electron and antineutrino, as illustrated in Figure 1. The reaction is as follows:

$$n \rightarrow p + e + \overline{\nu}_e \tag{1}$$

The quantum mechanical matrix element for neutron decay follows that for bare quarks:

$$\mathcal{M} = \left[G_V \overline{p}\, \gamma_\mu n - G_A \overline{p}\, \gamma_5 \gamma_\mu n \right] \left[\overline{e}\, \gamma^\mu (1 + \gamma_5) \nu \right], \tag{2}$$

but with constants G_V and G_A that give the relative strengths of the vector and axial vector contributions to the decay amplitude. According to the Conservation of Vector Current (CVC) hypothesis [1,2] $G_V = G_F V_{ud}$, where G_F is the universal weak coupling strength measured from muon decay and $V_{ud} = 0.97373 \pm 0.00031$ [3] is the first element of the Cabibbo–Kobayashi–Maskawa (CKM) quark mixing matrix in the Standard Model. However, the axial current is not conserved, so the value of G_A is influenced by the strong interaction of quarks within the neutron. Therefore, G_A must be determined experimentally from the neutron lifetime and neutron decay angular correlations. Including the latest radiative and other theoretical corrections, Czarnecki, Marciano, and Sirlin [4] found the relationship between G_A/G_V and the free neutron lifetime to be

$$\tau_n = \frac{4905.7(1.7)s}{|V_{ud}|^2\,(1+3(G_A/G_V)^2)}. \tag{3}$$

The neutron decay matrix element $\mathcal{M}$, expressed in Equation (2), determines more than just the neutron decay lifetime. It also governs many other charged-current weak interactions between free protons and neutrons that are important in astrophysics, solar physics, and cosmology. Therefore, the experimental value of the neutron lifetime plays an important role throughout physics.

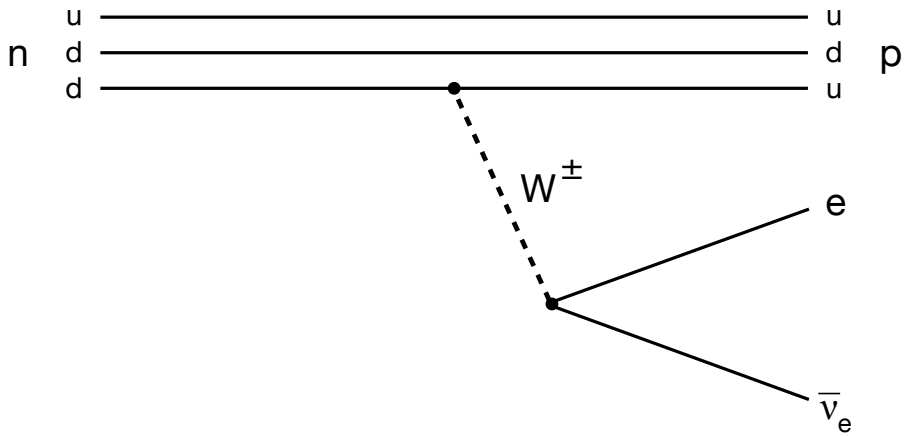

Figure 1. The Feynman diagram for free neutron decay.

3. Neutron Lifetime Experiments

The most precise experiments that measure the neutron lifetime fall into two main categories: *beam experiments*, where a slow neutron beam passes through an apparatus that simultaneously measures the rate of neutron decay via the decay products and the neutron beam density; and *ultracold neutron storage experiments*, where neutrons are slowed to a velocity that allows them to be stored, and the number that remains after some time is counted. Detailed historical reviews of neutron lifetime experiments can be found in [5,6].

3.1. Beam Method

The beam method is the oldest, presented by Robson in the first serious neutron lifetime measurement at the Chalk River reactor in 1950 [7], and improved and refined by later experiments over many decades. The most precise of these so far is the NIST BL1 experiment [8,9], producing the result $\tau_n = 887.7 \pm 2.2$ s (2013). The neutron decay rate $\dot{N}$ of a beam containing N neutrons in the fiducial decay region of the apparatus is given by the differential form of the exponential decay law

$$\dot{N} = -\frac{N}{\tau_n}. \tag{4}$$

The decay particles, protons and/or electrons, are counted by detectors in the apparatus at rate R_p, which is

$$R_p = -\varepsilon_p \dot{N} = \varepsilon_p \frac{A_{\text{beam}}\, L\, \rho_n}{\tau_n} \tag{5}$$

where ε_p is the detector counting efficiency, A_{beam} is the beam cross-sectional area, L is the length of the fiducial decay region, and ρ_n is the neutron density in the beam. To simplify this discussion, the beam is assumed here to have a uniform density and cross section. The density can be related to the neutron flux ϕ_n, the number of neutrons per unit area per unit time passing through some point in the beam, and the beam velocity v, using the usual formula $\phi_n = \rho_n\, v$. A typical high-flux slow-neutron beam has a broad velocity spectrum, so this becomes an integral:

$$\rho_n = \int \frac{\phi_n(v)}{v} dv. \tag{6}$$

where $\phi_n(v)$ is the *spectral flux*, i.e., the flux per neutron velocity. Combining Equations (5) and (6) provides

$$R_p = \varepsilon_p \frac{A_{\text{beam}}\, L}{\tau_n} \int \frac{\phi_n(v)}{v} dv. \tag{7}$$

Neutrons in the beam pass through a thin absorbing material downstream of the apparatus decay region and are either counted in real time via an (n, α) reaction in the absorber by detecting the alpha particles or by later measuring the neutron-induced radioactivity. Neutron absorption cross sections generally obey the $1/v$ law [10], with the few exceptions being materials with a very low energy absorption resonance, so the velocity-dependent absorption cross section can be written as

$$\sigma_{\text{abs}} = \frac{\sigma_{\text{th}}\, v_{\text{th}}}{v} \tag{8}$$

where σ_{th} is the tabulated thermal absorption cross section at the reference thermal velocity $v_{\text{th}} \equiv 2200$ m/s. The neutron count rate is then

$$R_n = \varepsilon_0 A_{\text{beam}} v_{\text{th}} \int \frac{\phi_n(v)}{v} dv. \tag{9}$$

where ε_0 is defined as the probability that a neutron at the reference velocity v_{th} that passes through the absorber will produce a detected count. It contains the thermal cross section σ_{th} and other efficiency factors such as the absorber thickness and the geometric efficiency of the alpha detectors. Combining Equations (7) and (9) provides

$$\tau_n = \frac{R_n\, \varepsilon_p\, L}{R_p\, \varepsilon_0\, v_{th}}. \tag{10}$$

Note that the spectral flux integrals divide out in this expression. In essence, the $1/v$ dependence of the neutron absorption cross section precisely compensates for the $1/v$ probability that the same neutron will decay inside the fiducial region, and so to excellent approximation the neutron lifetime result is independent of neutron velocity. Equation (10) seems simple enough, but precise absolute measurements of ε_p and ε_0 are very challenging. The fiducial length L is complicated by end effects where ε_p can be difficult to determine.

A schematic of the NIST BL1 experiment is shown in Figure 2. The neutron beam passed through a quasi-Penning trap, and when a neutron decayed inside it, the proton was trapped by the magnetic field and the electrostatic potential of the electrode array. At a specified frequency, typically about 100 Hz, the trap was opened by lowering the door electrodes to ground. Protons were then transported through a 9.5° bend in the magnetic field and accelerated into a silicon detector to be counted. The neutron rate was measured by counting alphas and tritons from the (n, α) reaction in a deposit of isotopically enriched

^{6}LiF on a thin silicon crystal wafer. An important feature of this experiment, along with its predecessor that ran at the Institut Laue-Langevin in France [11], is the segmented trap. The ratio R_n/R_p was measured as a function of trap length, and because the end effect was approximately constant for all trap lengths, it could be removed by means of extrapolation, greatly simplifying the determination of L. The neutron counting efficiency ε_0 was measured separately using an absolute neutron counting apparatus installed on a monochromatic neutron beam. Further details of the experiment and a thorough discussion of the systematic effects can be found in [8,9].

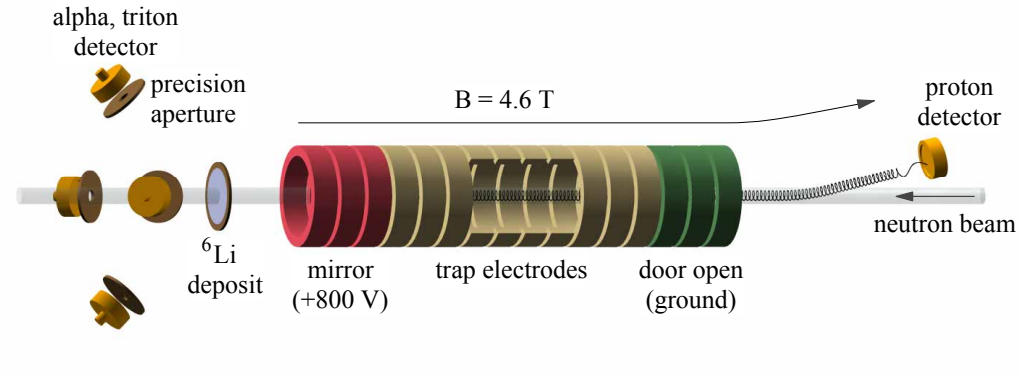

Figure 2. Scheme of the NIST BL1 beam neutron lifetime experiment [8,11]. The neutron beam passes through a proton trap. Decay protons are trapped axially by the door and mirror electrostatic potentials and radially by the axial magnetic field. They are counted periodically by lowering the door to the ground, as shown here. Neutrons are counted by detecting the alphas and tritons from the ^{6}Li (n,α) reaction in a thin deposit.

A new generation of the NIST beam experiment, called BL3, is currently being constructed and tested. It is a larger version of the apparatus that accommodates a much larger neutron beam (a factor of 25 larger area), with a new large-area segmented silicon proton detector. With these increases, the proton counting rate will be more than 100 times that of BL1. It incorporates several new features to improve, explore, and test systematic effects. BL3 is expected to complete commissioning in 2026 and begin running at NIST soon thereafter.

Another beam neutron lifetime experiment is currently running at J-PARC in Japan, with a method quite different from that of the NIST experiments. A pulsed neutron beam is admitted into a ^{3}He time projection chamber (TPC), where neutron decays are detected via ionization by the beta electrons, and the number of neutrons in the pulse is simultaneously measured via the $^3\mathrm{He}(n,p)^3\mathrm{H}$ reaction. The latest J-PARC result $\tau_n = 898 \pm 19$ s [12] agrees with the NIST BL1 result but with a large uncertainty. The J-PARC group is currently analyzing an improved dataset with an expectation of 3 s uncertainty, which could have a significant impact.

3.2. Ultracold Neutron Storage Method

Ultracold neutrons (UCNs) are neutrons with a kinetic energy at the order of 100 neV (velocity ~4 m/s). This is less than the neutron effective potential energy in some material surfaces, so UCNs will completely reflect from the walls of a suitably constructed bottle and can be stored for many minutes (various loss mechanisms limit the ultimate storage time). The gravitational potential energy of a neutron is 100 neV per meter, so UCNs can be confined vertically by gravity. The neutron magnetic dipole moment is 60 neV/T, so UCNs can be trapped in a strong inhomogeneous magnetic field. This ability to trap and store UCNs for long periods enables the measurement of the neutron decay lifetime by comparing the UCN population at different storage times. UCNs are admitted into the storage apparatus, the "UCN bottle", in a highly reproducible manner. After a storage time Δt, the surviving neutrons are extracted and counted by a neutron detector. At least two

storage times Δt_1 and Δt_2, typically one short and one long, are used. If neutron beta decay is the only means of losing neutrons from the bottle, then the neutron lifetime is obtained from the ratio N_1/N_2 of neutron counts following extraction.

$$\tau_n = \tau_{\text{storage}} = \frac{\Delta t_2 - \Delta t_1}{\ln(N_1/N_2)}. \tag{11}$$

In the presence of additional loss mechanisms, the observed neutron storage time τ_{storage} will be smaller than the beta decay lifetime τ_n, i.e.,

$$\frac{1}{\tau_{\text{storage}}} = \frac{1}{\tau_n} + \frac{1}{\tau_{\text{wall}}} + \frac{1}{\tau_{\text{quasi}}} + \frac{1}{\tau_{\text{other}}} \tag{12}$$

where τ_{wall} accounts for losses due to inelastic scattering and absorption on the bottle walls; τ_{quasi} is the average lifetime of "quasitrapped" UCNs that are not trapped but have trajectories that persist in the trap for a long time before escaping; and τ_{other} is due to other possible losses such as residual gas interactions. Many previous UCN storage experiments used material bottles, typically with hydrogen-free coatings such as Fomblin oil to reduce wall scattering. Still, elastic scattering from the walls dominated τ_{storage}, which as a result was much smaller than τ_n. By systematically varying the surface/volume ratio of the bottle and/or the UCN energy spectrum, both of which modulate the wall interaction rate, an extrapolation could be made to the zero scattering point.

More recent UCN storage experiments have used a magnetic "bottle", where permanent magnets are installed in a pattern that creates a strong field gradient near the wall. UCNs of one spin state (low field seekers) are strongly repelled by the field gradient and reflect off the wall with no material interaction, greatly reducing wall losses. Quasitrapped UCNs can be removed by means of a "cleaning" process that removes neutrons with kinetic energy close to the minimum trap potential. The most well known and successful of these is the UCNτ experiment at Los Alamos National Lab [13–15]. A schematic is shown in Figure 3. UCNs were polarized in a 5.5 T solenoidal magnet and spin-flipped into the low-field seeker state. They were then introduced through a trap door at the bottom of the storage volume to fill it. The storage volume, about 3 m long and 1 m high, was lined with a Halbach array of permanent magnets to reflect neutrons at the walls. UCNs were trapped vertically by gravity. An array of electromagnetic coils was used to maintain UCN polarization throughout the storage volume—a zero field point inside the volume can flip the spin of a neutron that passes through it, which will cause it to be ejected instead of reflected at the wall. After filling the storage volume, a cleaner was lowered to a specified height to remove, by means of scattering or absorption, all neutrons with sufficient mechanical energy to reach that height, in order to eliminate quasitrapped UCNs prior to commencing the storage period. Storage times from 20 s to over 1000 s were used. At the end of the storage period, surviving UCNs were counted in situ using a ^{10}B-coated ZnS scintillator detector lowered into the volume. The latest UCNτ result is the most precise reported neutron lifetime value to date: $\tau_n = 877.75 \pm 0.34$ s [15]. Systematic UCN loss mechanisms were sufficiently small that τ_{storage} (Equation (12)) was dominated by τ_n and no extrapolation was needed. An upgrade to the experiment, called UCNτ+, will introduce an adiabatic neutron "elevator" to load the trap more efficiently. It promises a factor of two reduction in uncertainty.

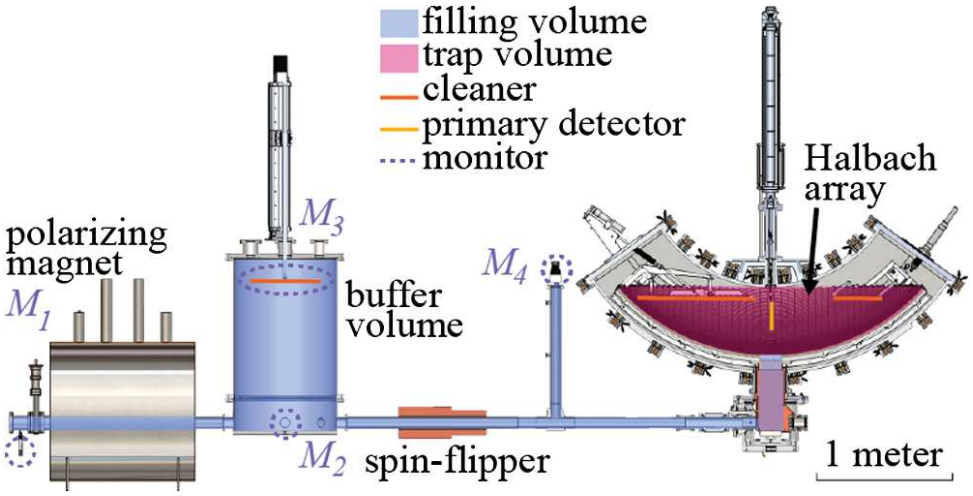

Figure 3. The Los Alamos UCNτ experiment [15]. UCNs are polarized in a superconducting solenoid (**left**), pass through a spin-flipper (**center**), and are admitted through a trap door into the storage volume (**right**) that is lined with a Halbach magnet array. UCNs are reflected only by magnetic and gravitational fields during the storage period, thus avoiding material interactions that result in neutron losses.

3.3. The Discrepancy

Figure 4 shows a summary of all neutron lifetime results with a reported uncertainty of less than 10 s. The three beam method results are in good agreement and their average $\tau_n = 888.1 \pm 2.0$ s is dominated by the updated NIST BL1 result [9]. There are nine UCN storage experiments represented here, with six using material bottles [16–21] and three using magnetic/gravitational storage [14,15,22], two of which are different runs of the UCNτ experiment described above. The nine UCN results are not in good agreement, with a reduced chi-squared $\chi^2_\nu = 3.34$, so the average $\tau_n = 878.36 \pm 0.45$ s has an error expanded by a factor of $\sqrt{\chi^2_\nu} = 1.83$. However the three magnetic/gravitational UCN storage experiments are in much better agreement; they average to $\tau_n = 878.15 \pm 0.20$ s. The difference between the beam method average and the UCN storage average (all nine experiments) is 9.8 ± 2.1 s, a discrepancy of more than four standard deviations. The difference between the beam method average and the magnetic/gravitational UCN storage average (three experiments) is 10.0 ± 2.0 s, which is slightly worse. Much has been written about this quite serious problem in the neutron lifetime. It is widely assumed that unknown or underestimated systematic errors in one or more of the experiments are responsible. However an exotic physics explanation remains possible (see Section 5). In particular, the NIST BL1 experiment has been carefully scrutinized due to its controlling effect on the beam average, but no smoking gun has been found so far (see [23–26] for more details). It is hoped that future experiments, both in progress and planned, will solve this problem and lead to a fully reliable value for the neutron lifetime.

Since 2019, the Particle Data Group has included only the "best eight" UCN storage results in their average for the recommended value of the neutron lifetime, $\tau_n = 878.4 \pm 0.5$ s [3], equivalent to the UCN average in Figure 4, but they note that if the NIST BL1 beam result is included in the average, the shift is rather small, to $\tau_n = 878.6 \pm 0.6$ s. In both cases, the errors include a $\sqrt{\chi^2_\nu}$ scale factor. As a practical matter, this is a reasonable approach, but it does not obviate the importance of resolving the discrepancy, which might result in a significant change to the recommended value.

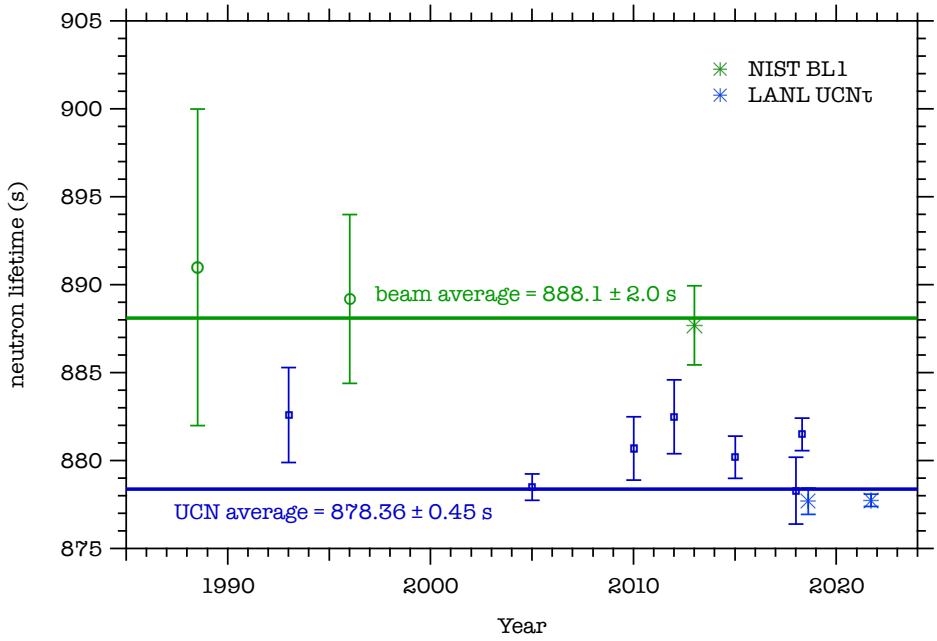

Figure 4. A summary of neutron lifetime experimental results with a reported uncertainty of less than 10 s. The averages of the beam method and UCN storage method results disagree by 9.8 ± 2.1 s. The UCN average uncertainty has been expanded by $\sqrt{\chi^2_\nu}$ due to poor agreement between the experiments. Beam experiment references: [9,11,27]. UCN storage experiment references: [14–22].

4. The Neutron Lifetime in Cosmology and Astrophysics

The Standard Big Bang Nucleosynthesis (SBBN) theory describes the formation of primordial light isotopes in the first few minutes following the Big Bang. Using the well-established Standard Model (SM) of particle physics, general relatively (GR), Λ cold dark matter Big Bang cosmology (ΛCDM), and only one free parameter, the baryon/photon ratio of the universe η, the SBBN theory predicts the relative abundances of ^{2}H and ^{4}He in very good agreement with modern astrophysical measurements. This success provides a remarkable confirmation of the SM, GR, and Big Bang cosmology. The basic ideas of the SBBN theory are described beautifully in the book *The First Three Minutes* by Weinberg [28]. For a recent scientific review, see Cyburt, Fields, Olive, and Yeh [29].

In the SBBN theory, free neutrons and protons condensed from the quark-gluon plasma in the period $t = 0.1$–100 ms, at a temperature $T \approx 10^{11}$ K. By $t = 100$ ms, essentially all free muons and pions had decayed. Protons and neutrons remained in thermal equilibrium with free leptons via weak interactions.

$$\begin{aligned} p + e &\longleftrightarrow n + \overline{\nu}_e \\ n + e^+ &\longleftrightarrow p + \nu_e. \end{aligned} \tag{13}$$

When the reaction rates of Equation (13), which scale with temperature as T^5, became less than the Hubble parameter, which scales as T^2, the density of particles was insufficient to maintain thermal equilibrium and nucleon "freeze out" occurred. This happened at $t \approx 1$ s, $T_{\rm freeze} \approx 10^{10}$ K ($k_B T_{\rm freeze} \approx 0.8$ MeV). At the time of nucleon freeze out, the ratio of neutrons to protons was set by the Boltzmann factor at the point just prior to leaving thermal equilibrium, i.e.,

$$n/p \approx \exp\left(-\frac{(m_n - m_p)c^2}{k_B T_{\rm freeze}}\right) = 0.17. \tag{14}$$

Neutrons and protons proceeded to form deuterons (^{2}H nuclei) via the reaction

$$n + p \longrightarrow d + \gamma \text{ (2.22 MeV)} \tag{15}$$

but due to the high value of the photon/baryon ratio $\eta^{-1} \approx 10^9$, the disintegration rate of deuterons exceeded the production rate until

$$\eta^{-1} \exp\left(-\frac{2.2\,\text{MeV}}{k_B T}\right) \approx 1 \tag{16}$$

or $T \approx 10^9$ K, at $t \approx 10$ s. After that, as the free deuteron density increased, the dominant reaction due to its large cross section was the formation of alpha particles via

$$d + d \longrightarrow \alpha + \gamma \text{ (23.9 MeV)}. \tag{17}$$

Other reactions also occured, but at much lower rates:

$$\begin{aligned} d + p &\longrightarrow {}^3\text{He} + \gamma \text{ (5.49 MeV)} \\ d + n &\longrightarrow {}^3\text{H} + \gamma \text{ (6.26 MeV)} \\ \alpha + {}^3\text{He} &\longrightarrow {}^7\text{Be} + \gamma \text{ (1.59 MeV)} \\ \alpha + {}^3\text{H} &\longrightarrow {}^7\text{Li} + \gamma \text{ (2.47 MeV)} \end{aligned} \tag{18}$$

By $t \approx 5$ min, virtually all primordial neutrons were bound within alpha particles (^{4}He nuclei), with trace amounts in the other nuclei on the right side of Equation (18). It took another 380,000 years for the universe to cool to the era where these nuclei could combine with free electrons to make neutral atoms. During that time, the primordial ^{3}H (τ = 12.3 y) and ^{7}Be (τ = 53.3 d) had all beta decayed into ^{3}He and ^{7}Li, respectively, leaving light hydrogen plus four primordial isotopes: ^{2}H, ^{3}He, ^{4}He and ^{7}Li. Due to the expansion/cooling rate of the universe, the mass 5, 8 barriers (there are no stable $A = 5$ or $A = 8$ isotopes), and the large Coulomb barriers for other reactions, nuclei heavier than the above did not form in the early universe; they had to wait millions of years for stellar processes to begin.

The primordial isotope abundance ratios, relative to hydrogen, have historically been calculated as a function of η. The latest measurements of the cosmic microwave background (CMB) by the Plank spacecraft have provided a sufficiently precise and robust value, $\eta = 6.104 \pm 0.055 \times 10^{-10}$ [30,31], for it to now be treated as an input parameter. Using this value, the abundances in Table 1 follow from the SBBN theory. Y_p and D/H are in excellent agreement with the observed ratios from astronomical measurements of emission lines in low-metallicity galactic and extragalactic clouds, which are expected to contain near-primordial abundances [32]. The agreement in D/H is particularly impressive and provides a powerful confirmation of the validity of the SBBN theory. The problem with ^{7}Li may be due to the stellar depletion of lithium. From the abundances in Table 1, we see that by $t \approx 5$ min, more than 99.99% of primordial neutrons were bound within ^{4}He nuclei. Therefore, the ^{4}He abundance ratio Y_p depends almost entirely on the n/p ratio during Big Bang nucleosynthesis.

Table 1. SBBN primordial isotope abundance ratios, using the latest CMB results for the baryon/photon ratio of the universe η, and a comparison to recent astronomical measurements [32].

Isotope Ratio	SBBN Prediction	Observed
$Y_p = {}^4\text{He/H}$	0.24691 ± 0.00018	0.2449 ± 0.0040
D/H	$2.57 \pm 0.13 \times 10^{-5}$	$2.55 \pm 0.03 \times 10^{-5}$
^{3}He/H	$10.03 \pm 0.90 \times 10^{-6}$	no data
^{7}Li/H	$4.72 \pm 0.72 \times 10^{-10}$	$1.6 \pm 0.3 \times 10^{-10}$

The neutron decay lifetime plays a key role here. The n/p ratio during nucleosynthesis depends strongly on the neutron lifetime in two ways: (1) the coupling constant factor $1 + 3(G_A/G_V)^2$ in Equation (3) gives the rate at which neutrons decay and also determines the strength of the reactions in Equation (13), and hence the temperature at which nucleon freeze out occurs which is the denominator in Equation (14); and (2) the n/p ratio decreases from freeze out to t = 5 min due to the decay of neutrons to protons. This dependence is nicely illustrated in Figure 5, which shows a scatter plot of SBBN-calculated Y_p values with input parameters varied according to their Gaussian uncertainties [32]. The 10 s neutron lifetime discrepancy covers almost the full horizontal range of this plot, so it is the biggest obstacle for a precise SBBN prediction for Y_p.

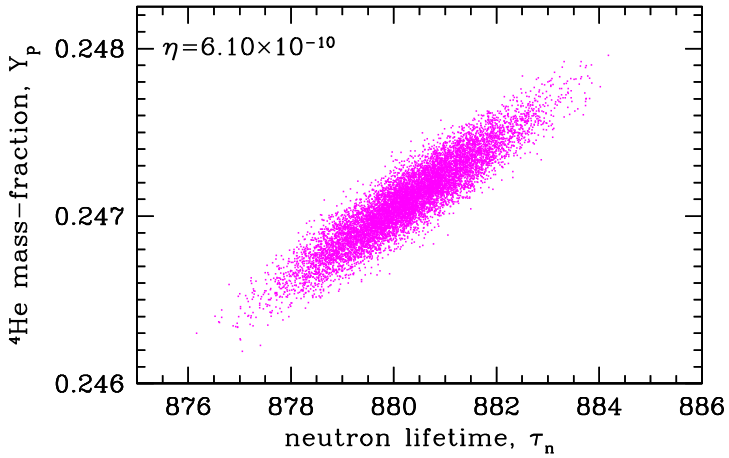

Figure 5. Results of a SBBN calculation (Cyburt, Fields, Olive, and Yeh [29]) showing the sensitivity of the primordial helium abundance Y_p to the neutron lifetime.

Another interesting approach to BBN is to treat the number of neutrino species as a free parameter rather than fixed at the Standard Model values $N_\nu = 3$ and $N_{\rm eff} = 3.046$, where N_ν is the number of actual neutrinos and $N_{\rm eff}$ includes the contribution to the radiation density of the universe caused by the distortion of the neutrino energy spectra by charged lepton annihilation and other possible degrees of freedom such as light WIMPs. Adding, hypothetically, the presence of more neutrino species increases the expansion rate of the universe, which leads to an increased freeze out temperature $T_{\rm freeze}$, which in turn shifts n/p and Y_p to larger values as per Equation (14). Using the Plank result $\eta = 6.104 \pm 0.055 \times 10^{-10}$, the PDG-recommended neutron lifetime $\tau_n = 878.4 \pm 0.5$ s, and the astronomical measurements of Y_p and D/H gives $N_\nu = 2.898 \pm 0.141$ [31] and $N_{\rm eff} = 2.94 \pm 0.19$ [29], both in good agreement with the Standard Model values. The neutron lifetime discrepancy has an unfortunate effect here as well. The 10 s discrepancy translates to $\Delta N_{\rm eff} \approx 0.19$, which is comparable to the present uncertainty in the calculation.

The neutron lifetime also plays an important role in stellar nucleosynthesis. In particular, the weak fusion reaction,

$$p + p \rightarrow^2 H + e^+ + \nu_e, \tag{19}$$

is a Gamow–Teller ($\Delta J = 1$) weak transition; a free proton in the initial state transforms into a neutron inside the spin-1 deuteron. The cross section contains the matrix element in Equation (2) and is proportional to the factor $1 + 3(G_A/G_V)^2$ in Equation (3), so it requires the neutron lifetime value as an input. The value of G_A/G_V also appears in calculations of other light element processes that are important in stellar physics, such as ^{8}B beta decay, responsible for the ^{8}B neutrino flux detected by the Homestake solar neutrino experiment [33].

5. The Neutron Lifetime and Dark Matter

Over the past decade, a number of very interesting ideas involving new physics have been proposed that could potentially explain the neutron lifetime discrepancy. Many of these rely on the fact that beam experiments measure the partial lifetime of Standard Model neutron beta decay, while UCN storage experiments measure the total lifetime of all neutron decay or disappearance modes, both known and unknown. If the neutron has an exotic, previously undetected, decay mode, then the UCN experiments would tend to measure a smaller lifetime. A prominent example is the suggestion by Fornal and Grinstein [34] that the neutron could decay into dark sector particles without inconsistency with previous experimental constraints. They considered the possibilities $n \rightarrow \chi\gamma$, $n \rightarrow \chi e^+e^-$, or $n \rightarrow \chi\phi$, where χ and ϕ are fermion and boson dark matter particles, respectively. The existence of massive neutron stars puts some pressure on this proposal [35–38], and the semi-visible modes with a photon or electron–positron pair in the final state have been excluded by subsequent experiments [39–41]. Another interesting suggestion [42] is that stored UCNs could be upscattered by the dark matter halo of the galaxy, which has a velocity relative to the Earth of ≈250 km/s. Very little energy transfer, ∼100 neV, is needed to remove UCNs from the storage volume, which would lead to an observed lifetime shorter than the beam neutron's lifetime.

Finally, mirror neutron oscillation has been considered as a possible explanation for the neutron lifetime discrepancy. A mirror sector that consists of a duplication of the known Standard Model particles, with minimal coupling with them other than gravity, has been proposed to explain the existence of dark matter [43]. If mirror neutrons n' have equal mass to ordinary neutrons n, and they couple very weakly, the oscillation transition time for $n \longleftrightarrow n'$ may be resonantly enhanced in a strong magnetic field by the dipole potential energy. The proton trap in the NIST BL1 experiment resides in a 4.6 T field, but the neutron absorber is in a low-field region, and therefore a resonant n-n' transition could cause the density of neutrons inside the trap to be lower than in the absorber, decreasing R_p relative to R_n in Equation (10) to produce a larger measured τ_n. A likely model for this was excluded by a recent experiment at Oak Ridge National Lab [44], but in general this idea remains viable.

6. Conclusions

The nearly 5-sigma beam-UCN discrepancy in the value of the free neutron lifetime is a significant outstanding problem that limits the precision of SBBN calculations and affects other astrophysical quantities. This problem is most likely due to underestimated systematic effects in the experiments and it will hopefully be resolved by current and future experimental efforts. But we should not neglect the possibility that this disagreement could be caused by new physics. While perhaps unlikely, a new physics explanation for the neutron lifetime discrepancy would have enormous consequences and may provide important clues as to the nature of dark matter.

Funding: This work was supported by National Science Foundation grant PHY-2309938.

Conflicts of Interest: The author declares no conflicts of interest in this work.

References

1. Feynman, R.P.; Gell-Mann, M. Theory of the Fermi Interaction. *Phys. Rev.* **1958**, *109*, 193. [CrossRef]
2. Gell-Mann, M. Test of the Nature of the Vector Interaction in Beta Decay. *Phys. Rev.* **1958**, *111*, 362. [CrossRef]
3. Particle Data Group; Workman, R.L.; Burkert, V.D.; Crede, V.; Klempt, E.; Thoma, U.; Tiator, L.; Agashe, K.; Aielli, G.; Allanach, B.C.; et al. Review of Particle Physics. *Prog. Theor. Exp. Phys.* **2022**, *2022*, 083C01.
4. Czarnecki, A.; Marciano, W.J.; Sirlin, A. Radiative corrections to neutron and nuclear beta decays revisited. *Phys. Rev. D* **2019**, *100*, 073008. [CrossRef]
5. Wietfeldt, F.E.; Greene, G.L. The neutron lifetime. *Rev. Mod. Phys.* **2011**, *83*, 1173. [CrossRef]
6. Wietfeldt, F.E. Measurements of the Neutron Lifetime. *Atoms* **2018**, *6*, 70. [CrossRef]
7. Robson, J.M. The Radioactive Decay of the Neutron. *Phys. Rev.* **1951**, *83*, 349. [CrossRef]

8. Nico, J.S.; Dewey, M.S.; Gilliam, D.M.; Wietfeldt, F.E.; Fei, X.; Snow, W.M.; Greene, G.L.; Pauwels, J.; Eykens, R.; Lamberty, A.; et al. Measurement of the neutron lifetime by counting trapped protons in a cold neutron beam. *Phys. Rev. C* **2005**, *71*, 055502. [CrossRef]
9. Yue, A.T.; Dewey, M.S.; Gilliam, D.M.; Greene, G.L.; Laptov, A.B.; Nico, J.S.; Snow, W.M.; Wietfeldt, F.E. Improved Determination of the Neutron Lifetime. *Phys. Rev. Lett.* **2013**, *111*, 222501. [CrossRef]
10. Amaldi, E.; D'Agostino, O.; Fermi, E.; Pontecorvo, B.; Rasetti, F.; Segré, E. Artificial Radioactivity produced by Neutron Bombardment. *Proc. R. Soc. Lond.* **1935**, *149*, 522.
11. Byrne, J.; Dawber, P.G.; Habeck, C.G.; Smidt, S.J.; Spain, J.A.; Williams, A.P. A revised value for the neutron lifetime measured using a Penning trap. *Europhys. Lett.* **1996**, *33*, 187. [CrossRef]
12. Hirota, K.; Ichikawa, G.; Ieki, S.; Ino, T.; Iwashita, Y.; Kitaguchi, M.; Kitahara, R.; Koga, J.; Mishima, K.; Mogi, T.; et al. Neutron lifetime measurement with pulsed cold neutrons. *Prog. Theor. Exp. Phys.* **2020**, *2020*, 123C02. [CrossRef]
13. Morris, C.L.; Adamek, E.R.; Broussard, L.J.; Callahan, N.B.; Clayton, S.M.; Cude-Woods, C.; Currie, S.A.; Ding, X.; Fox, W.; Hickerson, K.P.; et al. A new method for measuring the neutron lifetime using an in situ neutron detector. *Rev. Sci. Instr.* **2017**, *88*, 053598. [CrossRef] [PubMed]
14. Pattie, R.W., Jr.; Callahan, N.B.; Cude-Woods, C.; Adamek, E.R.; Broussard, L.J.; Clayton, S.M.; Currie, S.A.; Dees, E.B.; Ding, X.; Engel, E.M.; et al. Measurement of the neutron lifetime using a magneto-gravitational trap and in situ detection. *Science* **2018**, *360*, 627–632. [CrossRef] [PubMed]
15. Gonzalez, F.M.; Fries, E.M.; Cude-Woods, C.; Bailey, T.; Blatnik, M.; Broussard, L.J.; Callahan, N.B.; Choi, J.H.; Clayton, S.M.; Currie, S.A.; et al. Improved Neutron Lifetime Measurement with UCNτ. *Phys. Rev. Lett.* **2021**, *127*, 162501. [CrossRef] [PubMed]
16. Serebrov, A.P.; Kolomensky, E.A.; Fomin, A.K.; Krasnoshchekova, I.A.; Vassiljev, A.V.; Prudnikov, D.M.; Shoka, I.V.; Chechkin, A.V.; Chaikovskiy, M.E.; Varlamov, V.E.; et al. Neutron lifetime measurements with a large gravitational trap for ultracold neutrons. *Phys. Rev. C* **2018**, *97*, 055503. [CrossRef]
17. Mampe, W.; Bondarenko, L.; Morozov, V.; Panin, Y. Fomin, Measuring neutron lifetime by storing ultracold neutrons and detecting inelastically scattered neutrons. *J. Exp. Theor. Phys. Lett.* **1993**, *57*, 82.
18. Serebrov, A.; Varlamov, V.; Kharitonov, A.; Fomin, A.; Pokotilovski, Y.; Geltenbort, P.; Butterworth, J.; Krasnoschekova, I.; Lasakov, M.; Taldaev, R.; et al. Measurement of the neutron lifetime using a gravitational trap and a low-temperature Fomblin coating. *Phys. Lett. B* **2005**, *605*, 72. [CrossRef]
19. Pichlmaier, A.; Varlamov, V.; Schreckenbach, K.; Geltenbort, P. Neutron lifetime measurement with the UCN trap-in-trap MAMBO II. *Phys. Lett. B* **2010**, *693*, 221. [CrossRef]
20. Steyerl, A.; Pendlebury, J.; Kaufman, C.; Malik, S.; Desai, A. Quasielastic scattering in the interaction of ultracold neutrons with a liquid wall and application in a reanalysis of the Mambo I neutron-lifetime experiment. *Phys. Rev. C* **2012**, *85*, 065503. [CrossRef]
21. Arzumanov, S.; Bondarenko, L.; Chernyavsky, S.; Geltenbort, P.; Morozov, V.; Nesvizhevsky, V.; Panin, Y.; Strepetov, A. A measurement of the neutron lifetime using the method of storage of ultracold neutrons and detection of inelastically up-scattered neutrons. *Phys. Lett. B* **2015**, *745*, 79. [CrossRef]
22. Ezhov, V.F.; Andreev, A.; Ban, G.; Bazarov, B.; Geltenbort, P.; Glushkov, A.; Knyazkov, V.; Kovrizhnykh, N.; Krygin, G.; Naviliat-Cuncic, O.; et al. Measurement of the neutron lifetime with ultra-cold neutrons stored in a magneto-gravitational trap. *J. Exp. Theor. Phys. Lett.* **2018**, *107*, 707. [CrossRef]
23. Byrne, J.; Worcester, D.L. The neutron lifetime anomaly and charge exchange collisions of trapped protons. *J. Phys. G Nucl. Part. Phys.* **2019**, *46*, 085001. [CrossRef]
24. Byrne, J.; Worcester, D.L. The neutron lifetime anomaly: Analysis of charge exchange and molecular reactions in a proton trap. *Eur. Phys. J. A* **2022**, *58*, 151. [CrossRef]
25. Serebrov, A.P.; Chaikovskii, M.E.; Klyushnikov, G.N.; Zherebtsov, O.M.; Chechkin, A.V. Search for explanation of the neutron lifetime anomaly. *Phys. Rev. D* **2021**, *103*, 074010. [CrossRef]
26. Wietfeldt, F.E.; Biswas, R.; Caylor, J.; Crawford, B.; Dewey, M.S.; Fomin, N.; Greene, G.L.; Haddock, C.C.; Hoogerheide, S.F.; Mumm, H.P.; et al. Comment on "Search for explanation of the neutron lifetime anomaly". *Phys. Rev. D* **2023**, *107*, 118501. [CrossRef]
27. Spivak, P.E. Neutron lifetime obtained from Atomic-Energy-Institute experiment. *J. Exp. Theor. Phys.* **1988**, *67*, 1735.
28. Weinberg, S.L. *The First Three Minutes*; Basic Books: New York, NY, USA, 1993.
29. Cyburt, R.H.; Fields, B.D.; Olive, K.A.; Yeh, T.-H. Big Bang nucleosynthesis: Present status. *Rev. Mod. Phys.* **2016**, *88*, 15004. [CrossRef]
30. Planck Collaboration; Aghanim, N.; Akrami, Y.; Ashdown, M.; Aumont, J.; Baccigalupi, C.; Ballardini, M.; Banday, A.J.; Barreiro, R.B.; Bartolo, N.; et al. Planck 2018 results. VI. Cosmological parameters. *Astron. Astrophys.* **2020**, *641*, A6.
31. Yeh, T.H.; Shelton, J.; Olive, K.A.; Fields, B. Probing physics beyond the standard model: Limits from BBN and the CMB independently and combined. *JCAP* **2022**, *10*, 46. [CrossRef]
32. Fields, B.D.; Olive, K.A.; Yeh, T.H.; Young, C. Big-Bang Nucleosynthesis after Planck. *JCAP* **2020**, *3*, 10. [CrossRef]
33. Bahcall, J.N.; Davis, R., Jr. Solar Neutrinos: A Scientific Puzzle. *Science* **1976**, *191*, 264. [CrossRef]
34. Fornal, B.; Grinstein, B. Dark Matter Interpretation of the Neutron Decay Anomaly. *Phys. Rev. Lett.* **2018**, *120*, 191801. [CrossRef] [PubMed]
35. Cline, J.M.; Cornell, J.M. Dark decay of the neutron. *J. High Energy Phys.* **2018**, *2018*, 81. [CrossRef]

36. Motta, T.F.; Guichon, P.A.; Thomas, A.W. Implications of neutron star properties for the existence of light dark matter. *J. Phys. G* **2018**, *45*, 05LT01. [CrossRef]
37. Baym, G.; Heck, D.H.; Geltenbort, P.; Shelton, J. Testing Dark Decays of Baryons in Neutron Stars. *Phys. Rev. Lett.* **2018**, *121*, 061801. [CrossRef]
38. McKeen, D.; Nelson, A.E.; Reddy, S.; Zhou, D. Neutron Stars Exclude Light Dark Baryons. *Phys. Rev. Lett.* **2018**, *121*, 061802. [CrossRef] [PubMed]
39. Tang, Z.; Blatnik, M.; Broussard, L.J.; Choi, J.H.; Clayton, S.M.; Cude-Woods, C.; Currie, S.; Fellers, D.E.; Fries, E.M.; Geltenbort, P.; et al. Search for the Neutron Decay $n \to X + \gamma$, Where X is a Dark Matter Particle. *Phys. Rev. Lett.* **2018**, *121*, 022505. [CrossRef] [PubMed]
40. Sun, X.; Adamek, E.; Allgeier, B.; Blatnik, M.; Bowles, T.J.; Broussard, L.J.; Brown, M.A.-P.; Carr, R.; Clayton, S.; Cude-Woods, C.; et al. Search for dark matter decay of the free neutron from the UCNA experiment: $n \to \chi + e^+e^-$. *Phys. Rev. C* **2018**, *97*, 052501R. [CrossRef]
41. Klopf, M.; Jericha, E.; Märkisch, B.; Saul, H.; Soldner, T.; Abele, H. Constraints on the Dark Matter Interpretation $n \to \chi + e^+e^-$ of the Neutron Decay Anomaly with the PERKEO II Experiment. *Phys. Rev. Lett.* **2019**, *122*, 222503. [CrossRef]
42. Dawid, M. APS April Meeting 2022, session T12. Neutron-Axion Scattering and the Neutron Lifetime Puzzle. *Bull. Am. Phys. Soc.* **2022**, *67*, 6.
43. Berezhiani, Z.; Comelli, D.; Villante, F.L. The early mirror universe: Inflation, baryogenesis, nucleosynthesis and dark matter. *Phys. Lett. B* **2001**, *503*, 362. [CrossRef]
44. Broussard, L.J.; Barrow, J.L.; DeBeer-Schmitt, L.; Dennis, T.; Fitzsimmons, M.R.; Frost, M.J.; Gilbert, C.E.; Gonzalez, F.M.; Heilbronn, L.; Iverson, E.B.; et al. Experimental Search for Neutron to Mirror Neutron Oscillations as an Explanation of the Neutron Lifetime Anomaly. *Phys. Rev. Lett.* **2022**, *128*, 212503. [CrossRef] [PubMed]